Journal of Electrical Engineering & Technology Vol. 7, No. 3, pp. 429~435, 2012 **429**
http://dx.doi.org/10.5370/JEET.2012.7.3.429

An Approach for GPS Clock Jump Detection Using Carrier Phase Measurements in Real-Time

Youn Jeong Heo*, Jeongho Cho† and Moon-Beom Heo*

Abstract – In this study, a real-time architecture for the detection of clock jumps in the GPS clock behavior is proposed. GPS satellite atomic clocks have characteristics of a second order polynomial in the long term showing sudden jumps occasionally. As satellite clock anomalies influence on GPS measurements which could deliver wrong position information to users as a result, it is required to develop a real time technique for the detection of the clock anomalies especially on the real-time GPS applications such as aviation. The proposed strategy is based on Teager Energy operator, which can be immediately detect any changes in the satellite clock bias estimated from GPS carrier phase measurements. The verification results under numerous cases in the presence of clock jumps are demonstrated.

Keywords: GPS, Satellite clock anomaly, Clock jump detection, Teager energy

1. Introduction

Satellite signal anomalies reduce the user positioning performance of Global Navigation Satellite System (GNSS) applications [1]. In particular, if users obtain incorrect positioning from satellite signals with anomalies in crucial application areas such as in aviation, the accidents that may occur would cause great social impacts; and, it is essential that strict safety conditions be maintained [2].

Factors that may cause satellite signal anomalies include problems with the satellite itself, delays caused by the state of the troposphere and/or the ionosphere while satellite signals are being sent, and various other environmental influences. The signal anomalies resulting from these environmental factors include faults or anomalies related to the satellite clock, which can be called the heart of the satellite, as errors are fatal to users who rely wholly on the accuracy of Global Positioning System (GPS) measurements.

The GPS Master Control Station (MCS) checks the state of satellite clocks through the measurements obtained from 17 Monitor Stations, and it broadcasts the state of satellites in the navigation message to inform the users if the satellites are healthy or not. If any clock anomalies are originated, however, it is frequently the case that the MCS cannot detect and broadcast these anomalies in time to meet the user's requirements [3]. To meet the needs of signal integrity, augmentation systems such as the Local Area Augmentation System (LAAS) and Wide Area Augmentation System (WAAS) are being developed and deployed to address some of the shortcomings [4, 5]. Most of the studies in the augmentation systems are related to satellite integrity, however, and not specifically to that of the on-board clock. Therefore, this study focuses on methods of easily and quickly detecting satellite clock anomalies, particularly with respect to satellite clock jumps that affect GPS measurements.

Since frequency drifts are arisen over time in GPS satellite atomic clocks due to natural aging, the clocks involve clock bias with respect to the GPS Time (GPST), which behaviors have characteristics of a second order polynomial in the long term [6]. In addition, sudden anomalies such as phase jumps, frequency jumps, frequency increasing, etc., may also occur. Many studies have been conducted in order to detect these anomalies, observed in atomic clocks in ground station, which might be unlike behavior from what we intend to identify [7-11]. For example, Czopek applied a method that takes the average values of clock drifts in order to detect jumps that cause the average values to go out of a certain range, as in [7]. Wang and Rochat pursued a method to detect jumps using least square deviations and standard deviations [8]. Most of these methods involved obtaining the clock drifts for a certain time to find the time points at which the jumps occurred through differences from the average values or from the data fitting. However, these methods to detect jumps using average or fitting values are considering the clock drift behaviors, which are influenced by sample data's average size or the window width for data fitting. Therefore, the development of fast and accurate methods to detect satellite clock jumps in real time suitable to real time application areas is essential.

Teager Energy (TE) is a non-linear operator intended to measure the real physical energy of a system [12], which can immediately detect any changes that occur in signals.

† Corresponding Author: Dept. of Satellite Navigation, Korea Aerospace Research Institute, Korea.(jcho@kari.re.kr)
* Dept. of Satellite Navigation, Korea Aerospace Research Institute, Korea. (yjheo@kari.re.kr)
Received: January 1, 2011; Accepted: November 18, 2011

During the last twenty years of research, many applications have been developed using TE operator [13]-[15]. The most successful application so far has been demodulation of AM-FM signals, where we have seen particularly many applications in speech processing. Typically, Dunn *et al.* used the TE operator to detect transients in the background noise assumed to be slowly varying AM-FM signals, in addition to white noise [14]. Satellite atomic clocks work with high frequency stability in normal state, while the phase and frequency noise of the clocks have significant fluctuations in a malfunction. In this correspondence, we propose a simple and efficient methodology based on TE in order to immediately detect any sudden jump in real time in the drift phenomenon of satellite clocks. To assess the performance of the proposed method, The TE is applied to satellite clock biases estimated from GPS carrier phase measurements, and sudden jumps of several *ns* could be effectively detected from satellite clock drift behaviors ranging from several tens of *ns* to several hundred *ns* a day.

2. Teager Energy

Teager and Kaiser proposed non-linear operators intended to measure the energy of continuously oscillating signals in a single component. Equation (1) shows the energy operator for continuous time, while (2) shows the energy operator for discrete time [10].

$$E_C[x(t)] = \dot{x}^2(t) - x(t)\ddot{x}(t) \tag{1}$$

$$E_D[x(n)] = x^2(n) - x(n-1)x(n+1) \tag{2}$$

The motion of a mass m suspended by a spring of force constant k can be expressed as a simple oscillation signal given by $x(t) = A\cos(\omega t)$ where A is the amplitude of the oscillation and ω is the frequency of the oscillation, which is the same as $(k/m)^{1/2}$. The total energy of the oscillating object, which is the sum of kinetic energy and potential energy, is proportional not only to the square of the amplitude but also to the square of the frequency of the oscillation. If $x(n)$ is assumed to be samples of signals expressing the motion of the oscillating object, three samples can be combined to determine the values of amplitude and frequency, as shown in (3).

$$\begin{aligned} &x^2(n) - x(n+1)x(n-1) \\ &= A^2\sin^2(\Omega) \approx A^2\Omega^2 \end{aligned} \tag{3}$$

Since the energy in any single component signal is proportional to the squares of amplitude and frequency, the energy of the oscillation signal can be calculated by the difference between the square of the signal and the multiplication of the subsequent signals emitted, as shown in (2).

By applying the TE operator for discrete time to satellite clock biases to monitor changes in the energy, any changes occurring in the signals, such as jumps, can be immediately detected. Complicated functions containing two or more functions mixed together can be expressed by simple energy functions using TE, and thus, this nonlinear operator exhibits simplicity, efficiency, and ability to track instantaneously-varying special patterns in signals where various behaviors exist compositely, such as satellite clocks. In addition, by expressing the energy of oscillation signals, the characteristics of signals can be quantitatively expressed. This operator thus can be utilized effectively in comparing changes in signals. While general energy traditionally applies only signal magnitudes, TE considers both the amplitudes and frequencies of signals, which enables more effective detection of anomalies caused by changes in the amplitudes or frequencies of satellite clock signals.

In order to ensure the detection capability, therefore, TE was examined by processing a set of real GPS satellite clock data. As the real GPS satellite clock signal data cannot be acquired from the receiver, we took advantage of International GNSS Service (IGS) precise products that are the highest accuracy data in the alternative. The IGS creates and provides quite accurate clock solutions for satellites and individual stations by applying the weighted averages to the values obtained from eight analysis centers, which are determined on the basis of the IGS time linearly adjusted in relation to GPS time [16]. Note that the accuracy of the IGS precise clock solutions is 75 pico-seconds [17].

Fig. 1(a) and 1(b) shows the phase step and the Teager energy results of the satellite clock biases of PRN25 for 40 days, from 9 May (MJD 54960) to 18 June (MJD 55000) 2009, respectively. Since there were no clock anomalies during that period, the PRN25 satellite clock can be assumed to be operating in a benign condition. The data set of the phase step and the TE have a mean (μ) of 0.57 nano-seconds (ns) with a standard deviation (σ) of 0.03 ns and a zero-mean with a standard deviation of 0.02, respectively, as shown in the Table 1. The results of the satellites with poor quality data, such as PRN3, PRN8, PRN9, and PRN10, which satellites have cesium clocks, were not represented in the table. While the phase steps of all satellite clocks have different means with similar standard deviations, the TE have the zero mean with similar standard deviations.

The phase step is biased each according to frequency drift rate, as shown in the Fig. 1(a) and the alteration of mean complicates the anomaly detection strategy because threshold must be applied different in each time or each satellites. The other hand, the Teager energy results of each satellite are similar and it is convenience to realize the algorithm for the clock anomaly detection.

The probability distribution functions of the TE results have a Gaussian distribution. Even though the threshold

Table 1. Statistics of phase step and Teager energy results

	phase step		Teager energy	
PRN	μ	σ	μ	σ
2	0.02	0.07	-2.E-07	0.01
4	-0.47	0.11	7.E-07	0.01
6	0.43	0.05	4.E-07	0.01
7	-0.02	0.07	-2.E-07	0.00
11	-0.04	0.07	6.E-08	0.00
12	0.16	0.07	-1.E-06	0.03
13	0.03	0.06	-1.E-06	0.03
14	0.18	0.07	-9.E-07	0.01
15	-0.11	0.07	3.E-06	0.03
16	-0.10	0.07	5.E-07	0.01
17	0.06	0.07	-2.E-07	0.01
18	0.10	0.08	3.E-07	0.01
19	-0.04	0.07	2.E-06	0.00
20	-0.03	0.07	-8.E-07	0.01
21	-0.06	0.09	-3.E-07	0.00
22	-0.02	0.10	-2.E-07	0.02
23	0.00	0.07	-2.E-06	0.04
24	0.09	0.09	6.E-07	0.02
25	0.57	0.03	-9.E-06	0.02
26	0.03	0.04	4.E-07	0.00
27	0.10	0.17	5.E-08	0.01
28	-0.01	0.07	-2.E-07	0.00
29	0.11	0.06	-1.E-07	0.00
30	0.08	0.09	5.E-07	0.01
31	-0.02	0.07	-1.E-06	0.01
32	-0.16	0.02	-1.E-05	0.01

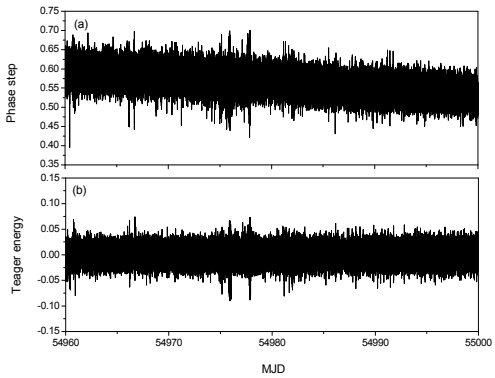

Fig. 1. Comparison of test results by phase step and Teager energy of PRN25 Clock

and probability of missed detection are not specified for the satellite clock, their effective paired values can be determined. Since the probability of normally distributed noise exceeding 6 σ is less than $1x10^{-8}$, the corresponding probability of missed detection < 1 $x10^{-8}$. In this study, the value of the probability of false alarm was set to $1x10^{-7}$, which is the same level of signal integrity level required for the Category I approach of airplanes [4], as shown in (4).

$$P_{FA} = 2\int_{Th}^{\infty} f(x)dx \approx 10^{-7} \tag{4}$$

Fig. 2 shows TE of PRN26 when supposed a jump of 0.25 ns occurred to 12h on May 3 (MJD 54954), which corresponds to extent of 5 σ of phase step of rubidium of PRN26. It is shown that the jump phenomenon is detected effectively.

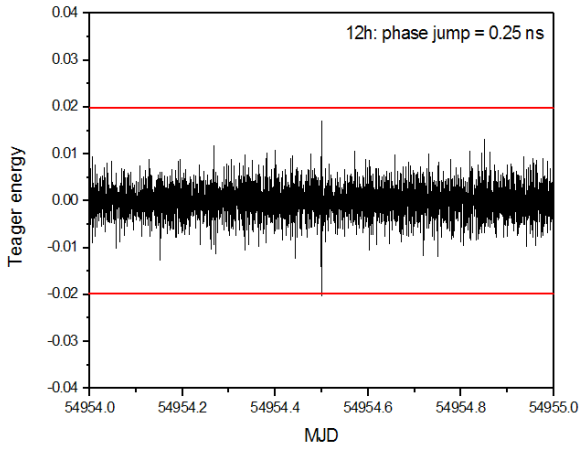

Fig. 2. Teager energy results of PRN26 occurred a phase jump at 12h.

3. GPS Clock Jump Detection Methodology

The GPS carrier phase measurements of the i^{th} satellite can be modeled as follows:

$$\begin{aligned} \Phi_{L1} &= \rho + c(B_A - B^i) - I_{L1} + T + \lambda_{L1}N_{L1} + \varepsilon_{\phi_{L1}} \\ \Phi_{L2} &= \rho + c(B_A - B^i) - I_{L2} + T + \lambda_{L2}N_{L2} + \varepsilon_{\phi_{L2}} \end{aligned} \tag{5}$$

where Φ_{L1} and Φ_{L2} are the carrier phase measurements at the L1 and L2 frequencies, respectively; ρ is the range between the position of satellite i and the position of receiver A; B_A and B^i is the receiver clock and the satellite clock biases, respectively, relative to GPST; I and T are the ionospheric and tropospheric propagation delays, respectively; N and λ are the integer ambiguity and the wavelength of the L1 and L2 frequencies, respectively, and ε is the receiver measurement noise. GPS provides two types of measurements: code phase and carrier phase measurements for positioning and timing. In general, as the code phase data involve larger measurement errors as compared to the carrier phase measurements, satellite clock jumps would be detected in a better way when using carrier phase data.

Fig. 3 is a block diagram illustrating the proposed strategy for detecting satellite clock jumps using GPS carrier phase measurements. Prior to detecting satellite clock anomalies, satellite clock bias should be estimated. The satellite clock bias, B^i, can be extracted only after accurately removing error factors other than satellite clocks among those included in the GPS measurements, as shown in (5). Subsequently, TE enables the detection of the satellite clock anomalies representing an energy value

surpass a certain threshold.

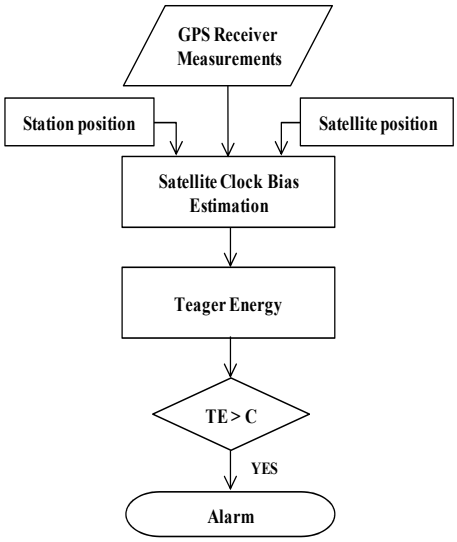

Fig. 3. Process of detecting satellite clock jumps using GPS carrier phase measurements

The ionospheric propagation delays, I, are phenomena caused by the number of free electrons in the path of a signal, defined as the total electron content (TEC), and can be modeled as varying inversely with the carrier frequency, f_L, squared as

$$I_L = -\frac{40.3TEC}{f_L{}^2} \tag{6}$$

In the case of utilizing a single frequency receiver, ionospheric delay errors are estimated using one of ionospheric models , e.g., the Klobuchar model, and it is generally known that the errors can be corrected by up to 50%. Furthermore, the ionospheric delay terms in the carrier phase measurements in (5) can be effectively removed by using the measurements of dual frequencies [18]; the ionospheric errors are removed by linearly combining dual frequency measurements represented by (7).

$$\Phi_{L3} = \frac{1}{f_{L1}^2 - f_{L2}^2}[f_{L1}^2\Phi_{L1} - f_{L2}^2\Phi_{L2}] \tag{7}$$

The tropospheric delays, T for satellite i take the form:

$$T = -(d_{hyd} + d_{wet}) \cdot m(el) \tag{8}$$

where d_{hyd} and d_{wet} are the estimated range delays for a satellite at 90° elevation angle, caused by atomospheric gases in hydrostatic equilibrium and by water vapor, respectively; $m(el)$ is a mapping function to scale the delays to the actual satellite elevation angle (el). Models for the tropospheric delays include the Saastamoinen model, Hopfield model, Magnavox model, and Collins model [19]. For the estimation of the range delays, d_{hyd} and d_{wet} in (8), Collins model employs five atmospheric factors—pressures, temperatures, water vapor pressures, temperature change rates, and water vapor change rates—by considering seasonal changes and the latitudes and heights of receivers, and thus more accurate tropospheric delays can be obtained as compared to other models.

In the case of determining the range, ρ, from satellite i to receiver A, satellite position errors might be created due to the inaccuracy of satellite orbital ephemerides. In particular, ephemerides, which are included in navigation messages, have an accuracy of 100 m. Therefore, the ultra-rapid orbit solutions provided by the IGS, which have an accuracy of 10 cm, are used to obtain the precise satellite position in this paper.

Since GPS receivers generally use oscillators with low grade specifications, receiver clock biases serve as the largest error source among GPS error components. Although receiver clock errors can be corrected taking measurements received from different satellites, they can be effectively removed if the receivers are synchronized by atomic clocks, which have a comparable performance to satellite clocks. Hence, in this study, data from receivers synchronized by atomic clocks are utilized in order to enhance the accuracy of satellite clock error estimation.

Fig. 4 illustrates a configuration intended to obtain GPS measurements in real time as well as clock jump detection architecture at the same time. The GPS receiver is synchronized with an atomic clock; it can reduce the effect of receiver clock errors in determining satellite clock biases. Its antenna installed on the rooftop is covered with choking, and this helps reduce multiple path errors, so that multiple path error are not considered. Then, the satellite clock biases are estimated once the range from receiver A to satellite i, receiver clock biases, and tropospheric delay are removed from the Φ_{L3} measurements, as in (9).

$$cB^i = -(\Phi_{L3} - \rho - cB_A - T) + N_{L3} + \varepsilon_{\Phi_{L3}} \tag{9}$$

$$N_{L3} = \frac{cf_{L1}N_{L1} - cf_{L2}N_{L2}}{f_{L1}^2 - f_{L2}^2} \tag{10}$$

The initial unknown integer of the carrier phases is not considered and copied with the initial clock bias estimated from code measurements since it is a constant as in (10).

After all the errors addressed are corrected TE is considered to detect satellite clock anomalies. By applying the TE operator for discrete time to the satellite clock biases to monitor changes in the energy, as shown in (11), any changes occurring in the signals, such as jumps, can be immediately detected.

$$E[B] = \dot{B}^2 - B\ddot{B} \tag{11}$$

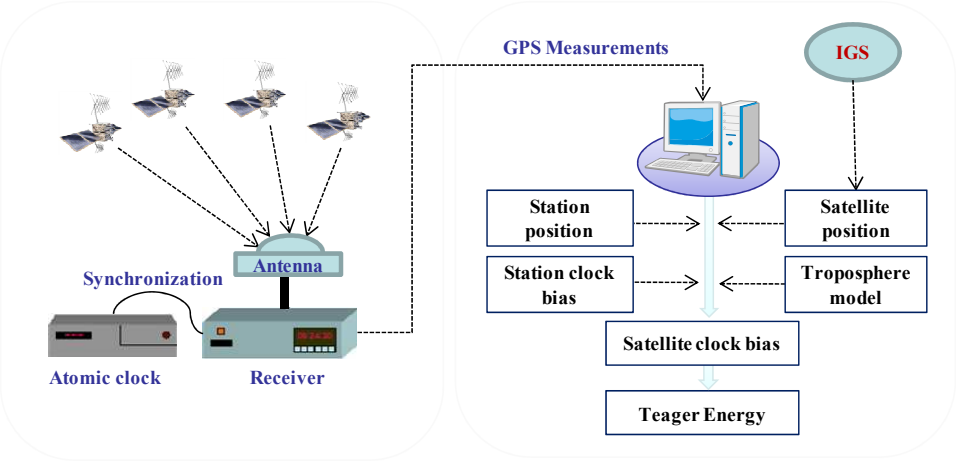

Fig. 4. Architecture for satellite clock jump detection in real time

Since the satellite clock drift occurs continuously over time, TE shows beyond the threshold despite no clock anomaly if the signal is lost and regained, and thus the TE is ignored in the case.

4. Experimental Results

Before applying the satellite clock jump detection methods to the GPS measurements, the satellite clock products provided by the IGS were examined in order to accurately identify the satellite clocks where jumping phenomena occurred and the time points at which the jumps occurred. In this study, we utilized the satellite clock biases at intervals of 30 s in CLOCK RINEX format. For 2 years, from January 1, 2008 to December 31, 2009, we used 32 satellites including satellites PRN01 through PRN32 in order to identify satellite clock jumps. Table 3 indicates the satellites which have demonstrated clock jump phenomena and the time point of the occurrence. Fig. 5(a) shows PRN25 satellite clock bias and Fig. 5(b) is clock residuals, which are remaining errors after removing drift effects, obtained from IGS clock products. As seen in Fig. 5(b), it can be identified that approximately 10 *ns* jumping phenomenon occurred on June 18, 2009 (MJD 55000) in PRN25. In addition, as shown in Fig. 4, we have observed clock jumping phenomena from other satellites and identified June 15, 2009 (MJD 54997) in PRN30.

Through the IGS precise satellite clock bias, the satellite in which the clock jumping phenomena occurred and the time point of the occurrence were identified. Then, the developed satellite clock jump detection method was applied to the satellite in which the clock jumping phenomena occurred with the observed GPS data at the time point of the occurrence to check the possibility of detecting satellite clock anomalies in real time.

The observed data from the satellites with the clock jumping phenomena reviewed above were obtained from

Table 2. GPS Satellites where clock jump phenomena observed from IGS

PRN	Year	DOY	Clock Jump Point			
			MJD	hour	min	sec
4	2009	310	55141.90382	21	41	30
5	2008	324	54789.86354	20	43	30
8	2009	109	54940.44063	10	34	30
24	2008	178	54643.73646	17	40	30
25	2009	169	55000.63368	15	12	30
30	2009	166	54997.7066	16	57	30
32	2009	110	54941.81979	19	40	30

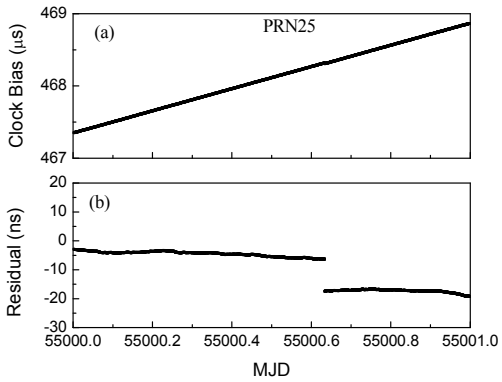

Fig. 5. PRN25 satellite clock jump in IGS clock products

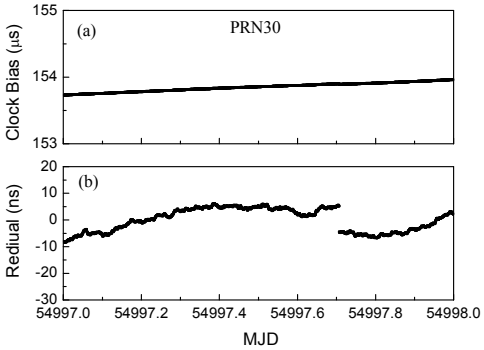

Fig. 6. PRN30 satellite clock jump in IGS clock products

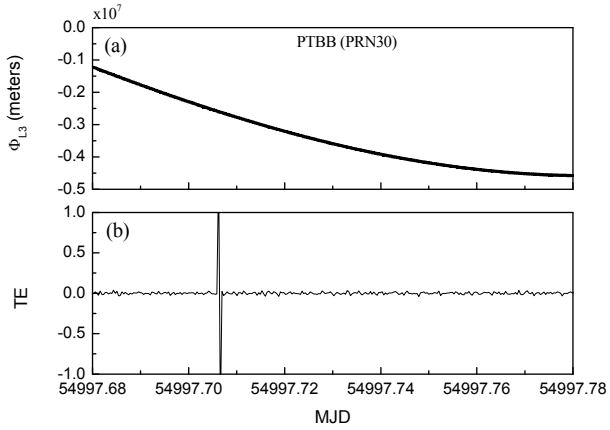

Fig. 7. PRN30 satellite clock jump detection with the GPS carrier phase measurements received from the PTB reference station: (a) Ionosphere-free carrier phase measurements; (b) Teager energy results.

Table 3. Facts on the GPS monitoring stations

Station	Receiver type	External clock
KRISS	Ashtech Z-XII3T	H-MASER
PTB	Ashtech Z-XII3T	CESIUM
USNO	Ashtech Z-XII3T	H-MASER

KRISS (Korea Research Institute of Standards and Science), USNO (US Naval Observatory), and PTB (Physikalisch- Technische Bundesanstalt), which receivers are synchronized by stable standard reference clocks as shown in Table 3, and applied to the proposed satellite clock anomaly monitoring architecture. The receiver position was determined using the predefined coordinates by using precise positioning methods, and the satellite positions were determined using the IGS ultra-rapid solutions.

Fig. 7 shows the resultant satellite clock jumps detected from the GPS carrier phase measurements corresponding to MJD 54997, where the jumping phenomenon of PRN 30 occurred. In the Fig. 7, (a) is the ionosphere-free carrier phase measurements (Φ_{L3}) combining dual frequency measurements and (b) is the Teager Energy using the carrier phase measurements where it can be seen that the clock jump instance identified is same as observed in Fig. 4. Also, it should be noted that even if the carrier phase measurements seen in Fig. 7(a), which contains a clock jump, do not show any anomalous behavior, it is evident that it is certainly capable of detecting jumping phenomena with the proposed detection scheme. In addition, we have performed the assessment of the proposed clock jump identification scheme with the data from PRN32 as well as PRN04 and the results illustrated in Fig. 8 and Fig. 9 have shown once again that it is able to detect the instance of occurrence of clock jumps satisfactorily.

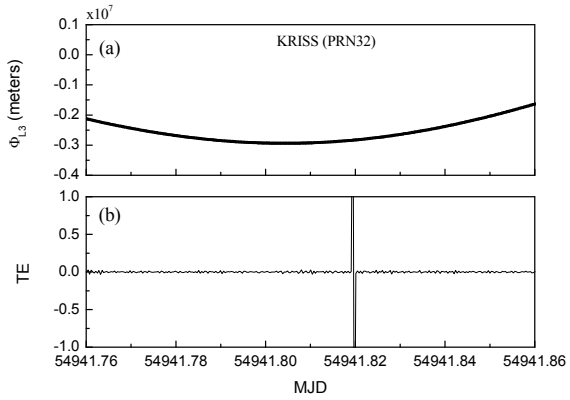

Fig. 8. PRN32 satellite clock jump detection with the GPS carrier phase measurements received from the KRISS reference station: (a) Ionosphere-free carrier phase measurements; (b) Teager energy results.

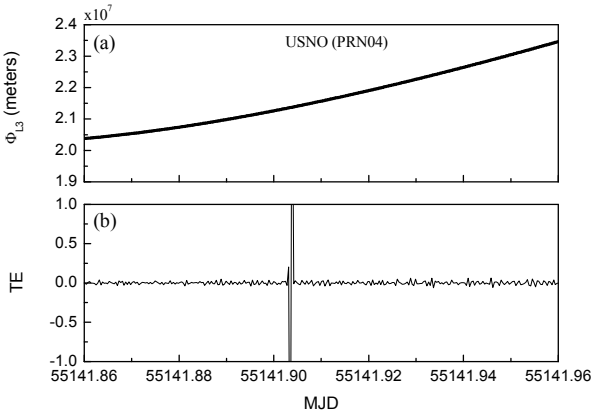

Fig. 9. PRN04 satellite clock jump detection with the GPS carrier phase measurements received from the USNO reference station: (a) Ionosphere-free carrier phase measurements; (b) Teager energy results.

5. Conclusion

Since sudden satellite signal anomalies are causes of considerable errors in those application areas where precise positioning in real time is required, such as in airplane take-offs and landings, technologies that can detect and supplement satellite signal anomalies in real time, such as RAIM, WAAS, or LAAS, have been developed and are in operation; however, technologies that can enhance the ability to detect and quickly respond to satellite signal anomalies are continuously required.

In this study, in order to solve the problems that arise in detecting satellite clock anomalies, which are difficult to solve with existing methods in real time, a method incorporating the TE with estimated satellite clock bias information obtained from GPS measurements observed in real time was presented. To identify the usefulness of the proposed method, the TE was applied to satellite clock biases estimated from carrier phase measurements, and as a

result, sudden jump of several *ns* occurred in satellite clock tendencies flowing around several tens of *ns* ~ several hundred *ns* a day could be captured. The applicability of the TE in detecting satellite clock anomalies in real time will be extended into a new study to apply the proposed method to real time application areas.

Acknowledgements

This work was supported by the Korea Research Council of Fundamental Science & Technology. The authors would like to thank their colleagues in the timing laboratories for granting the use of their GPS observations data.

References

[1] A. Hansen, T. Walter, P. Enge and D. Lawrence, "GPS satellite clock event SVN 27 and its impact on augmented navigation systems," *in Proceedings of ION GPS-98*, Nashville, Tennessee, September 1998.

[2] ICAO, ICAO Annex 10, *International Standards and Recommended Practices, Aeronautical Telecommunications*, vol. I, Radio Navigation Aids, 2001.

[3] P. Misra and Per Enge, *Global Positing System: Signal, Measurement, and Performance*, Ganga-Jamuna Press, 2001.

[4] RTCA, *Minimum Aviation System Performance Standards for LAAS*, RTCA DO-245, Washington DC, USA, 2004.

[5] RTCA, *Minimum Operational Performance Standard for GPS/WAAS Airborne Equipment*, RTCA DO-229c, Washington DC, USA, 2001.

[6] J. Phelan, T. Dass, G. Freed, J. Rajan, J. D'Agostino and M. Epstein, "GPS block IIR clocks in space: current performance and plans for the future," *in Proceeding of 37th PTTI Meeting*, Vancouver, Canada, August 2005.

[7] S. Czopek, "Frequency and phase break detection," *in Proceeding of 41st PTTI Meeting*, New Mexico, USA, November 2009.

[8] Q. Wang and P. Rochat, "An anomaly clock detection algorithm for a robust clock ensemble," *in Proceeding of 41st PTTI Meeting*, New Mexico, USA, November 2009.

[9] E. Nunzi, L. Galleani, P. Tavella and P. Carbone, "Detection of Anomalies in the Behavior of Atomic Clocks," *IEEE Transactions on Instrumentation and Measurement*, vol. 56, no. 2, pp.523-528, 2007.

[10] W. Riley, "Algorithms for Frequency Jump Detection," *Metrologia*, vol. 45, pp.154-161, 2008.

[11] L. Galleani and P. Tavella, "Detection and identification of atomic clock anomalies," *Metrologia*, vol. 45, pp.127-133, 2008.

[12] J. Kaiser, "On a Simple Algorithm to Calculate the Energy of a Signal," *in Proceeding of ICASSP*, New Mexico, USA, April 1990.

[13] P. Maragos, "On Amplitude and Frequency Demodulation Using Energy Operators," *IEEE Transactions on Signal Processing*, vol. 41, no. 4, pp.1532-1550, 1993.

[14] R. Dunn, T. Quatieri and J. Kaiser, "Detection of Transient Signals Using the Energy Operator," *in Proceeding of ICASSP*, Minnesota, USA, April 1993.

[15] R. Hamila, M. Renfors, M. Gabbouj and J. Astola, "Time-frequency signal analysis using Teager energy," *in Proceeding of 4th ICECS*, Cairo, Egypt, December 1997.

[16] K. Senior, P. Koppang, D. Matsakis and J. Ray, "Developing an IGS Time Scale," *IEEE Transactions on Ultrasonics, Ferroelectrics, and Frequency Control*, vol. 40, pp.585-593, 2003.

[17] IGS website, http://igscb.jpl.nasa.gov/

[18] B. Parkinson and J. Spilker, *The Global Positioning System: Theory and Applications*, AIAA, Washington, DC, 1996.

[19] J. Farrell and M. Marth, *The Global Positioning System and Inertial Navigation*, Mcgraw-Hill, 1999.

Youn Jeong Heo She received her Ph.D. degree in Space Science from Chungbuk National University, Korea, in 2010. She is a senior researcher in the Satellite Navigation team, Korea Aerospace Research Institute (KARI). Her research interests include GPS satellite signal anomaly detection, GPS time transfer, and precise point positioning system.

Jeongho Cho He received his Ph.D. degree in Electrical and Computer Engineering from the University of Florida, Gainesville, FL, in 2004. He joined Samsung Electronics in 2006, after one year appointment as a postdoctoral research associate at the University of Florida. Since 2008, he has been a senior researcher in KARI where he is investigating on FDE approaches, with applications on satellite navigation.

Moon-Beom Heo He received M.S. and Ph.D. degrees in Mechanical and Aerospace Information Engineering from Illinois Institute of Technology, U.S. in 1997 and 2004. He is the head of the Satellite Navigation team, CNS/ATM and Satellite Navigation Research Center in Korea Aerospace Research Institute (KARI). His research interests include GNSS-based navigation system including Ground Based Augmentation System (GBAS).